ELSEVIER

Applied Acoustics, Vol. 48, No. 1, pp. 15–32, 1996
Copyright © 1996 Elsevier Science Ltd
Printed in Great Britain. All rights reserved
0003-682X/96/$15.00 + 0.00

0003-682X(95)00040-2

Active Noise Control of Enclosed Harmonic Fields by Using BEM-Based Optimization Techniques

Mingsian R. Bai & Sernshen Chang

Department of Mechanical Engineering, National Chiao Tung University, 1001 Ta Hsueh Road, Hsin Chu 30050, Taiwan

(Received 12 January 1995; revised version received 27 June 1995; accepted 27 June 1995)

ABSTRACT

Boundary element methods (BEM) in conjunction with optimization algorithms are employed for active noise control of sound fields in three-dimensional enclosures. Total time-averaged acoustic potential energy is chosen as the cost function for the optimization procedure. The BEM is used to model the monochromatic sound field generated by noise sources in the enclosure. The constrained steepest descent method proves to be effective when both positions and amplitudes of the secondary sources are to be optimized, while the direct matrix inversion, the steepest descent method, and the conjugate gradient method prove to be useful when only the amplitudes of secondary sources are to be optimized. The developed BEM-based optimization techniques are applied to control the noise in a rectangular enclosure and a vehicle cabin.

Keywords: Boundary element method, optimization algorithms, enclosed harmonic fields, active noise control.

INTRODUCTION

Active noise control (ANC) involves the use of secondary sources to attenuate the sound field generated by the primary source. There has been a vast amount of literature on the subject of ANC.[1] Nelson and Elliott[2] calculated the optimal monopole amplitude of a secondary source in the free field by minimizing the total power output. Tohyama and Suzuki[3] used the modal expansion technique to minimize the power output of a monopole in an enclosure. It was demonstrated that the power output can be reduced to zero if the secondary source is very close to the primary source. Nelson *et al.*[4] proposed another ANC method for free-field noise

sources. In another paper,[5] the same authors attempted to calculate the optimal positions of the secondary sources, based on the total time-averaged acoustic potential energy in an enclosed monochromatic noise field. It was found that, above the Schroeder's cut-off frequency, the distance between the primary source and secondary source must be less than half a wavelength. Elliott *et al.*[6] investigated active minimization of the total power output and active absorption of sound. Recently, Cunefare and Koopmann[7] developed an ANC method based on boundary element methods (BEM) for the noise output near the surfaces and in the far field of extended radiators.

In this study, we seek to perform ANC of the noise field radiated by noise sources in enclosures with known normal specific acoustic impedance. The direct BEM is employed for modeling. In optimization schemes, the total time averaged acoustic potential energy is chosen as the cost function. The constrained steepest descent method is used if both the positions and amplitudes of the secondary sources are to be optimized. The direct matrix inversion algorithm, the steepest descent algorithm, and the conjugate gradient algorithm are used if only optimal amplitudes of secondary sources (at prescribed positions) are of concern. In a simulation, a rectangular enclosure with known analytical solution and a vehicle cabin of complex geometry are selected to verify the developed techniques.

It is pointed out by the reviewer that two existing papers by Molo and Bernhard[8,9] are closely related to this study. However, the major advances of this paper in comparison with the previous work are that this research emphasizes more the optimization schemes, e.g. the constrained steepest decent method. In addition, a vehicle cabin is used as a more realistic test case to illustrate the necessity and versatility of BEM.

THE MODELING TECHNIQUE

From linear acoustics, a monochromatic sound field containing N point sources can be described by[10]

$$(\nabla^2 + k^2)p(\mathbf{x}) = \sum_{j=1}^{N} s_j \delta(\mathbf{x} - \mathbf{x}_j), \tag{1}$$

where k is the wave number, s_j is the amplitude of the jth source, $\mathbf{x}$ is the position vector of the field point, $\mathbf{x}_j$ is the position vector of the jth point source, and δ is the Dirac delta function. Assume that the enclosure is bounded with the surfaces of known normal specific acoustic impedance $z_n = -i\rho ck\beta$, where ρ is the density of medium, c is the speed of sound, $\beta = \rho/(\delta p/\delta n)$, $i = -1$, and $\delta p/\delta n = n \cdot \nabla \rho$ is the directional derivative with n being the unit outward normal to the boundary.

From Green's function theory, the solution to the boundary-value problem in eqn (1) reads

$$\alpha(\mathbf{x}_p)p(\mathbf{x}_p) = \sum_{j=1}^{N} S_j \frac{e^{ik|\mathbf{x}_p - \mathbf{x}_j|}}{4\pi|\mathbf{x}_p - \mathbf{x}_j|}$$

$$+ \int_S \left[G(\mathbf{x}_p, \mathbf{x}_q) \frac{\partial}{\partial n_q} p(\mathbf{x}_q) - p(\mathbf{x}_q) \frac{\partial}{\partial n_q} G(\mathbf{x}_p, \mathbf{x}_q) \right] dS \tag{2}$$

$$\alpha(\mathbf{x}_p) = \begin{cases} 1, & \mathbf{x}_p \in V \\ \Omega(\mathbf{x}_p)/4\pi, & \mathbf{x}_p \in S, \\ 0, & \mathbf{x}_p \notin V \end{cases}$$

where $\Omega(\mathbf{x}_p)$ is the solid angle at the point $\mathbf{x}_p$, V is a volume bounded by the surface S, and $G(\mathbf{x}_p, \mathbf{x}_q) = \exp(ikr)/4\pi r$ is the three-dimensional free-space Green's function satisfying

$$(\nabla^2 + k^2)G(\mathbf{x}_p, \mathbf{x}_q) = -\delta(\mathbf{x}_p - \mathbf{x}_q) \tag{3}$$

where $\mathbf{x}_p$ and $\mathbf{x}_q$ denote the field point and the source point, respectively, and

$$r = |\mathbf{x}_p - \mathbf{x}_q|$$

In this study, discretization of boundary integral equation is done by means of isoparametric transformation.[11] Dividing the boundary into N_e elements with N_n nodes, taking the field points to the boundary, and carrying out nodal collocation, we may rewrite eqn (2) into the following matrix form:

$$\mathbf{Sp} = \mathbf{Ap}_n - \mathbf{Bp} + \mathbf{c} \tag{4}$$

$$\text{where } \mathbf{A} = [A_{mn}] = \left[\sum_{e=1}^{N_e} \left\{ \int_{S^{(e)}} G(\mathbf{x}_{pm}, \mathbf{x}_q(\xi)) |\mathbf{J}(\xi)| \, \mathbf{H}(\xi) \, dS \right\} \right] \tag{5}$$

$$\mathbf{B} = [B_{mn}] = \left[\sum_{e=1}^{N_e} \left\{ \int_{S^{(e)}} \nabla G(\mathbf{x}_{pm}, \mathbf{x}_q(\xi)) \cdot \mathbf{n}_q(\xi) |\mathbf{J}(\xi)| \mathbf{H}(\xi) \, dS \right\} \right] \tag{6}$$

$$\mathbf{c} = [c_m] = \left[\sum_{j=1}^{N} s_j \frac{e^{ik|\mathbf{x}_{pm} - \mathbf{x}_j|}}{4\pi|\mathbf{x}_{pm} - \mathbf{x}_j|} \right] \tag{7}$$

where $\mathbf{S}$ is an $N_n \times N_n$ diagonal matrix whose diagonal terms are composed of $\Omega(\mathbf{x}_p)/4\pi$, $\mathbf{p}$ and $\mathbf{p}_n$ are the acoustic pressure vector and its gradient vector on the surface, respectively, $\xi = (\xi_1, \xi_2)$ are the natural coordinates, $\mathbf{H}(\xi)$ is a row vector with shape function as its components, $\mathbf{J}(\xi)$ is the Jacobian matrix associated with the coordinate transformation, and $m, n = 1, 2, ..., N_n$.

On the other hand, the impedance-type boundary condition is expressed as

$$\mathbf{p}_n - \mathbf{R}\mathbf{p} = 0 \tag{8}$$

where $\mathbf{R} = \text{diag}(1/\beta_1, 1/\beta_2, ..., 1/\beta_{Nn})$. Thus eqn (4) can be reduced to

$$[(\mathbf{S} + \mathbf{B}) - \mathbf{A}\mathbf{R}]\mathbf{p} = \mathbf{c} \tag{9}$$

If the surface pressure is solved from eqn (9), then the pressure at the field point can be recovered from eqn (2).

OPTIMIZATION TECHNIQUES

To attenuate the sound field generated by noise sources, we choose to find the optimal control by secondary sources that minimizes the following total time averaged acoustic potential energy in the enclosure:[1]

$$E_p = \frac{1}{4\rho c^2} \int_V |p(\mathbf{x})|^2 \, dV \tag{10}$$

This function basically sums the squared pressures at all points within the enclosure.

Various types of constraints are incorporated into the optimization algorithm. For instance, one may require the secondary sources to be confined within the enclosure and the monopole amplitudes to be within a certain limit, i.e.

$$\begin{aligned} &\mathbf{x}_j \in D, \quad j = 1, 2, ..., M \\ &|s_j| < s_{\max}, \quad j = 1, 2, ..., M \end{aligned} \tag{11}$$

where s_j is the amplitude of the jth source, M is the number of secondary sources, $s_{\max}$ is the maximum amplitude of secondary sources, and D denotes the geometric extent of the enclosure. An additional constraint that may arise in practice is that, due to the physical sizes of acoustic sources, the distance between the primary source and secondary source may be within a certain number, i.e. $|r| > \varepsilon$.

To solve the above constrained optimization problem, the constrained steepest descent (CSD) method was adopted.[12] This method requires the following Pshenichny's descent function $\Phi(\mathbf{z})$ to monitor the progress of the algorithm towards the optimum:[13]

$$\Phi(\mathbf{z}) = f(\mathbf{z}) + QV(\mathbf{z}) \tag{12}$$

where $\mathbf{z}$ is the vector of design variables, $f(\mathbf{z})$ is the original cost function, Q is a positive number called the penalty parameter, and $V(\mathbf{z}) \geq 0$ is the maximum constraint violation.

The optimization process iteratively updates the position vector $\mathbf{z}$ by the following recursive formula:

$$\mathbf{z}^{(k+1)} = \mathbf{z}^{(k)} + t_k \mathbf{d}^{(k)} \tag{13}$$

where $\mathbf{d}^{(k)}$ is the search direction at the point $\mathbf{z}^{(k)}$ and t_k is the acceptable step size at $\mathbf{d}^{(k)}$. Next, the search direction $\mathbf{d}$ is obtained by solving the quadratic programming subproblem.[13] At the kth iteration, one determines an acceptable step size t_j, j being the smallest integer satisfying the descent condition

$$\Phi_{k+1,j} \leq \Phi_k - t_j \beta_k; \quad j = 0, 1, 2, \ldots . \tag{14}$$

The constant β_k is determined by the search direction $\beta_k = \gamma |\mathbf{d}^{(k)}|^2$, where γ is a constant between 0 and 1.

In general, it is not an easy task to find the global minimum in a highly non-linear problem. To obviate this difficulty, a Bayesian criterion is employed to determine if the local minimum found by CSD is possibly the global minimum.[13] Let r be the number of random samples that converge, after n points have been sampled, to the same region near a local minimum $\tilde{F}$. The Bayesian criterion states that the probability for which the local minimum $\tilde{F}$ found by CSD is actually the global minimum F^* is bounded from below as

$$\Pr[F = F^*] \geq q(n, r) = 1 - \frac{[(n+1)!(2n-r)!]}{[(2n+1)!(n-r)!]} \tag{15}$$

In the study, 0.98 was selected as the threshold. Namely, if the calculated value of $q(n, r)$ is greater than 0.98, then the result is regarded as the global minimum.

Evidently, the implementation of the total time-averaged acoustic potential energy requires a large number of sensors to detect the sound pressures throughout the enclosure. It is more desirable to restrict the number of sensors and to focus only on some quiet zones, e.g. the vicinity of the ears of a car driver. A further simplification can be done by optimizing only the amplitudes of secondary sources at prescribed positions. This is a reasonable approach since the optimal amplitudes of secondary sources are generally more difficult to determine than the positions, which will become clear shortly. In addition. the amplitude constraint in eqn (11) is also removed to simplify the optimization problem into a fully unconstrained type. Let the complex pressure output from the lth sensor e_l be the superposition of the complex pressure d_l due to the primary source and the pressure due to the M secondary sources. By writing the complex amplitude of the mth secondary source as y_m, the total output from the lth sensor can be expressed as[1]

$$e_l + d_l + C_{l1}y_1 + C_{l2}y_2 + C_{l3}y_3 + ... + C_{lM}y_M \tag{16}$$

where the frequency response function C_{lm}, $m = 1, 2, ..., M$, is determined by measuring the complex pressure output of the lth sensor with the mth secondary source operating alone, leaving all the other sources inactive. In matrix notation

$$\mathbf{e} = \mathbf{d} + \mathbf{C}\mathbf{y} \tag{17}$$

Here, the cost function can be defined as the sum of the squared moduli of the pressure outputs from all sensors

$$J = \frac{V}{4\rho c^2 L} \sum_{l=1}^{L} |e_l|^2 = \frac{V}{4\rho c^2 L} \mathbf{e}^H \mathbf{e} \tag{18}$$

In general, the number of sensors L must not be less than the number of the secondary sources M in order to admit an overdetermined problem. For this quadratic cost function, there exists a unique solution[1]

$$\mathbf{y}_0 = -(\mathbf{C}^H \mathbf{C})^{-1} \mathbf{C}^H \mathbf{d} \tag{19}$$

which leads to the minimum cost function

$$J_0 = \frac{V}{4\rho c^2 L}\mathbf{e}^H\left[\mathbf{I} - \mathbf{C}(\mathbf{C}^H\mathbf{C})^{-1}\mathbf{C}^H\right]\mathbf{d}$$

If the elements of **d** and **C** are calculated in advance by using BEM, then the optimal amplitudes of the secondary sources can be determined via eqn (19). This approach is referred to as the direct matrix inversion algorithm.

In practice, ill-conditioned problems may arise when two columns of the matrix $\mathbf{C}^H\mathbf{C}$ are very similar due to, for example, poor positioning of the secondary sources. This motivates the use of iterative methods such as the steepest descent method and the conjugate gradient method to optimize the amplitudes of the secondary sources.[12] Both methods require definition of a complex gradient g_j for the jth element

$$g_j = \frac{J}{\delta y_{jR}} + i\frac{\delta J}{\delta y_{jI}} \tag{21}$$

where y_{jR} and y_{jI}, are the real part and imaginary part of y, respectively. In the optimization process, the amplitudes of the secondary sources are iteratively updated by the following recursive formula:

$$\mathbf{y}^{(k+1)} = \mathbf{y}^{(k)} + t_k\mathbf{d}^{(k)} \tag{22}$$

where $\mathbf{y}^{(k)}$ and $\mathbf{y}^{(k+1)}$ are the amplitudes of the secondary sources at the kth and the $(k+1)$th iterations, respectively, $\mathbf{d}^{(k)}$ is the search direction at the kth iteration, and t_k is the step size at the kth iteration.

The direction of steepest descent (i.e. the negative gradient) is computed at the design point

$$\mathbf{d}^{(k)} = -\mathbf{g}^{(k)} \tag{23}$$

where $\mathbf{g}^{(k)}$ is the complex gradient defined in eqn (21) at the kth iteration. If $\mathbf{d}^{(k)}$ is a non-zero vector, the design point is moved along that direction with a proper step size to reduce the cost function. Although the procedure is simple, in some cases convergence may be excessively slow for practical applications.

Another attractive approach that provides faster convergence than the steepest descent method is the conjugate gradient method. This method incorporates a scaled direction vector of the last iteration into the current direction of steepest descent.

$$\mathbf{d}^{(k)} = -\mathbf{c}^{(k)} + \mu_k\mathbf{d}^{(k-l)} \tag{24}$$

where $\mathbf{c}^{(k)} = \mathbf{g}^{(k)}$ $\mathbf{d}^{(0)} = -\mathbf{g}^{(0)}$ and $\mu_k = (\| \mathbf{c}^{(k)} \| / \| \mathbf{c}^{(k-1)} \|)^2$.

In the steepest descent algorithm and the conjugate gradient algorithm, either constant step sizes or dynamic step sizes can be used. Dynamic step sizes corresponding to the largest reduction of cost function along the search direction can be determined by the method of golden section search.[12] This amounts to the minimization of

$$f(\mathbf{y}^{(k)} + t\mathbf{d}^{(k)})\bar{f}(t) \tag{25}$$

with respect to the step size t.

COMPUTER SIMULATION

Rectangular enclosure

A 3 m × 2 m × 1 m rectangular enclosure is selected for the computer simulation, as shown in Fig. 1. The origin is located at the center of the rectangular enclosure whose boundary is divided into 22 elements with 68 nodes.

In this simulation, a special type of impedance boundary condition is adopted.[8] It is well known that acoustic resistance contributes to acoustic damping and reduces the resonant peak, while the acoustic reactance slightly alters the resonant frequencies from those of the rigid-walled enclosure. In this study, acoustic reactance was chosen to be a constant for simplicity and the acoustic resistance is assumed to be inversely proportional to the frequency. That is, the acoustic impedance z_n is expressed as $\mu/k + i\eta$, where μ and η are constants.

The total time averaged acoustic potential energy defined in eqn (10) is selected as the cost function that is evaluated by using 24-point trapezoidal integration (see Fig. 2). Consider a case where only a primary source is present in the rectangular enclosure. It is desired to control the noise field by using one secondary source. Assume that the position of the primary source is (1.5, 0.5, 0.2), the amplitude of the primary source is 1, the wave

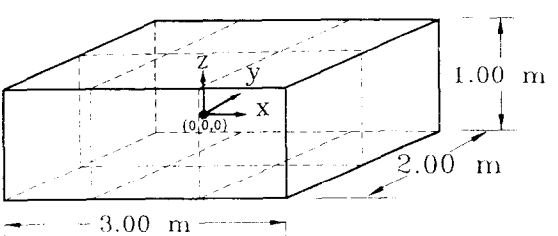

Fig. 1. Dimensions of the rectangular enclosure in which the origin is located at the center of the enclosure.

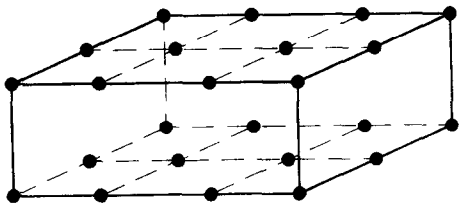

Fig. 2. Locations of 24 sensors for the trapezoidal rule integration of E_p in the rectangular enclosure.

number is 1, and the amplitude of the secondary source must not exceed 10. By CSD, the optimal amplitude is found to be -1.01 and the optimal position is found to be (1.49, 0.50, 0.19) for the secondary source. The relative positions of the primary source and the secondary source are shown in Fig. 3(a). The primary source and the secondary source form a dipole, which conforms to the conclusion of Tohyama and Suzuki.[3] On the other hand, if the distance between the primary source and the secondary source is constrained to be greater than 0.2 m, the optimal amplitude is found to be -1.02 and the optimal position is found to be (1.48, -0.45, 0.17) for the secondary source. The relative positions of the primary source and the secondary source under the distance constraint are shown

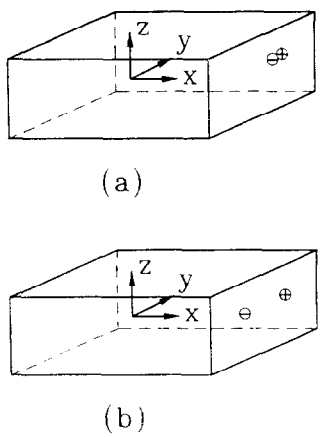

Fig. 3. The optimal positions of the secondary sources for the rectangular enclosure. The primary source of unity amplitude ($k = 1$) is located at (1.5, 0.5, 0.2). The boundary impedance z_n is $10^5/k + 10^5 i$. The amplitude of secondary source must not exceed 10. (a) The optimal position of the secondary source is found to be (1.49, 0.50, 0.19) without the distance constraint $|r| > 0.2$ and the optimal amplitude of the secondary source is found to be -1.01; (b) the optimal position of the secondary source is found to be (1.48, -0.45, 0.17) with the distance constraint $|r| > 0.2$ and the optimal amplitude of the secondary source is found to be -1.02.

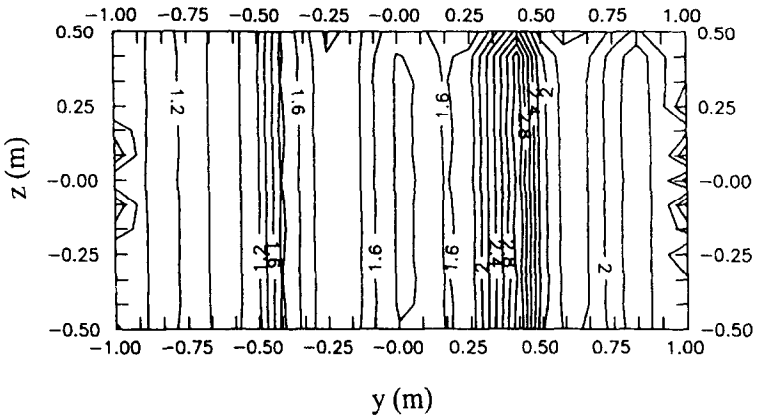

Fig. 4. The pressure amplitude in the plane $x = 1.5$. The primary source of unity amplitude ($k = 1$) is located at (1.5, 0.5, 0.2). The boundary impedance z_n is $10^5/k + 10^5 i$.

in Fig. 3(b). The optimal position of the secondary source appears to be nearly the mirror image of the primary source about the $y = 0$ plane. These interesting results can be easily explained by examining the pressure distribution in the enclosure. A contour plot of the sound pressure magnitude in the plane $x = 1.5$ is shown in Fig. 4. The local maxima are along $y = \pm 0.5$ lines. Without the constraint $|r| > 0.2$, the secondary source is located near the first pressure maximum ($y = 0.5$ line), while with the constraint $|r| > 0.2$, the secondary source is located near the second pressure maximum ($y = 0.5$ line). Thus, a conclusion can be drawn from the above result that the secondary sources are preferably located at pressure antinodes to obtain the best possible noise attenuation. Effective ANC can usually be accomplished, especially in the vicinity of resonant frequencies, unless the secondary sources happen to be placed at the pressure nodes. This is illustrated by the following simulation case. Figure 5 shows the effects of the positions of the secondary sources on ANC. In this case, the primary source is located at (1.0, 0.2, 0.2). J is chosen as the cost function and three sensors are used in the case. The method of direct matrix inversion is used to calculate the optimal ANC. It is observed that the noise reduction at resonant frequencies achieved by the secondary source located at (−1.4, −0.9, −0.4) is larger than the noise reduction achieved by the secondary source located at (0, 0.15, 0.15) for the (1, 0, 0) mode ($k = 1.04$). This is due to the fact that the secondary source located at (0, 0.15, 0.15) coincides with the pressure node of (1, 0, 0) mode. It is difficult for the secondary source at this position to excite the (1, 0, 0) mode. In control terminology, the secondary source at this position has very poor controllability on the noise field.

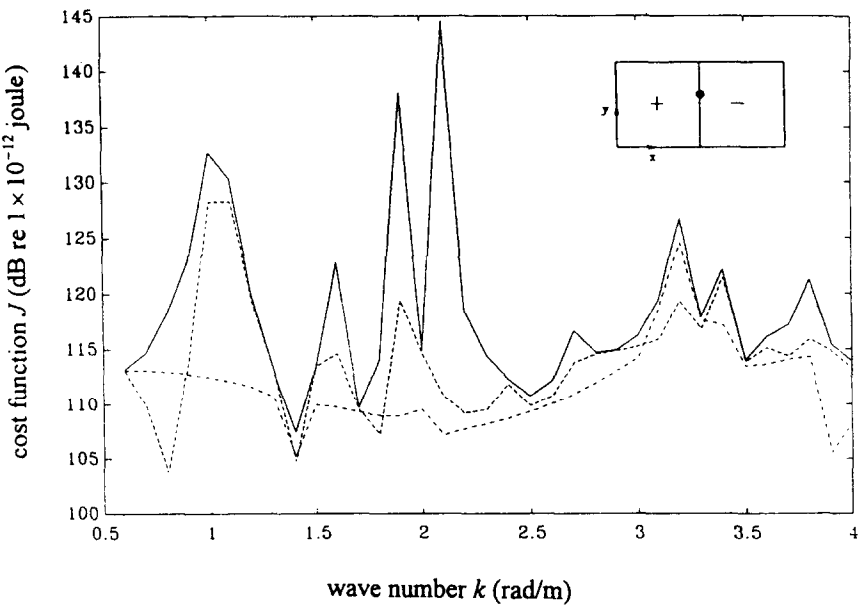

Fig. 5. The effect of the positions of secondary sources on ANC. The primary source of unity amplitude is located at (1.0, 0.2, 0.2). The boundary impedance z_n is $10^5/k + 10^5 i$. Three sensors are located at (1.4, 0.95, 0.45), (1.5, 0.4, 0.2) and (0.2, 0.1, 0.1). The mode shape of (1,0,0) mode ($k = 1.04$) is shown in the upper right corner of the illustration. ———, uncontrolled field; - - -, secondary source located at (0, 0.15, 0.15); – · –, secondary source located at (−1.4, −0.9, −0.4)).

Excellent noise reduction has been achieved in the frequency range 27.29–218.36 Hz, even though the distance between the primary source and the secondary source is greater than half a wavelength. For instance 6 dB noise reduction is obtained at $k = 4$ rad/ms where the distance between the primary source and the secondary source (1.32 m) is greater than half a wavelength (0.79 m). This is in contrast with the situations for frequencies above the Schroeder's cut-off (2.75 kHz at $k = 4$), where good noise reduction can only be obtained for the distances between the primary source and the secondary source less than half of a wavelength.

As already mentioned, it is preferably to place the sources at the pressure antinodes. Thus, in what follows, we concentrate on optimization of the amplitudes of secondary sources at prescribed positions. Consider a case in which the primary source of unity amplitude is located at the origin and the secondary source is located at (1.5, 0.2, 0.2). Three sensors are used to monitor the noise field. Table 1 shows the results of optimal amplitudes of the secondary sources calculated by direct matrix inversion, conjugate gradient method, and steepest descent method, with constant and variable dynamic sizes. It is observed that a significant reduction in

TABLE 1

The results of ANC when only the amplitudes of secondary sources are to be optimized. The primary source of unity amplitude ($k=1$) is located at the origin. The secondary sources are located at (1.5, 0.2, 0.2) and (1.0, 1.0, 0.3), and the sensors are located at (−1.5, 0.1, 0.2) and (−1.5, 0.4, 0.2). The initial guesses of the amplitudes of the secondary sources are $0.1232+0.2241i$ and $0.7650+0.6774i$. The boundary impedance z_n is assumed to be $10^5/k+10^5 i$. The following results are obtained after 200 iterations

Optimization method	J	J_0	*Amplitude*	*CPU time(s)*
Direct matrix inversion	0.12	0	$-0.7421+0.5072i$ $0.1960-0.0429i$	32.04
Steepest descent with constant step size 0.01	0.12	1.23×10^{-4}	$-0.6543+0.0703i$ $-0.1592-0.3804i$	1979.34
Steepest descent with dynamic step size	0.12	1.19×10^{-5}	$-0.4092+0.7000i$ $-0.1297-0.2593i$	1157.34
Conjugate gradient with constant step size 0.01	0.12	2.61×10^{-5}	$-0.4536+0.1053i$ $-0.1592+0.3804i$	1845.13
Conjugate gradient with dynamic step size	0.12	2.30×10^{-11}	$-0.7238+0.5468i$ $0.1858-0.0533i$	208.45

the cost function has been achieved by these three methods. For the iterative methods, the conjugate gradient method converges faster than the steepest descent method. The iterative methods with dynamic step size converge faster than the methods with constant step size.

The position of sensors is another important issue for noise control. In the following case, the primary source of unity amplitude is located at (1.0, 0.2, 0.2) and the secondary source is located at (−1.4,−0.9, −0.4). J is chosen as the cost function. Three sensors are used to monitor the sound field and one of them can be moved to examine the effects of different locations of sensors. We chose to place the movable sensor at (1.45, 0.95, 0.45) and (1.0, 0.1, 0.2), respectively, where the former is a corner point and the latter is an interior point. Figure 6(a) and (b) show the noise reduction obtained by positioning the sensors at the corner point and at the interior point, respectively. The noise reduction in Fig. 6(a) appears more pronounced than the reduction in Fig. 6(b). In control terminology, the sensors located in the pressure anti-nodes (that are usually around corners) have good observability.

In the following example, the effect of the number of secondary sources on ANC is also investigated. The sound field is controlled by one, two and three secondary sources, respectively. J is chosen as the cost function. The primary source is located at (1.0, 0.2, 0.2). Four sensors are used in this case. As can be seen from the results in Fig. 7, the more secondary sources, the greater is the noise reduction.

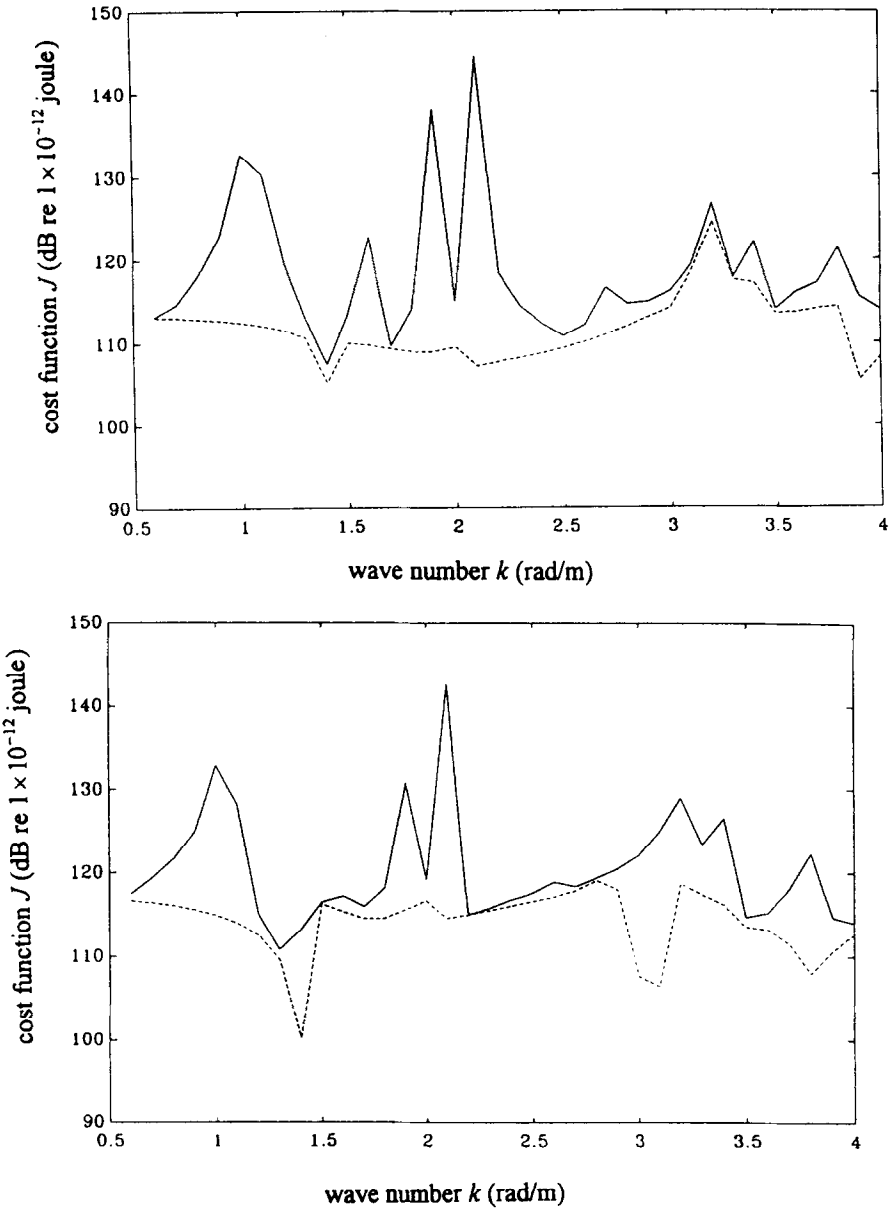

Fig. 6. The effect of the positions of sensors on ANC. The boundary impedance z_n is $10^5/k+10^5i$. The primary source of unity amplitude is located at (1.0, 0.2, 0.2). The secondary source is located at (−1.4, −0.9, −0.4). Two sensors are located at (1.0, 0.4, 0.2) and (0.2, 0.1, 0.1). (a) The third sensor at (1.45, 0.95, 0.45) is located near the corner of the enclosure; (b) the third sensor at (1.0, 0.1, 0.2) is located in interior of the enclosure. ——— , uncontrolled field; - - -, controlled field.

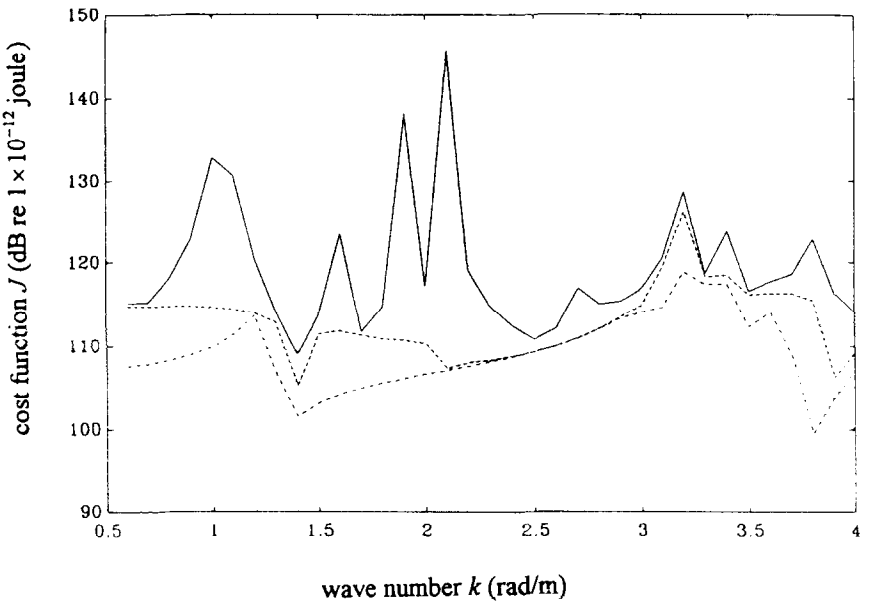

Fig. 7. The effect of the number of secondary sources. The boundary impedance z_n is $10^5/k + 10^5 i$. The primary source of unity amplitude is located at (1.0, 0.2, 0.2). Four sensors are located at (1.4, 0.95, 0.45), (1.5, 0.4, 0.2), (0.2, 0.1, 0.1) and (−0.3, −0.2, −0.15).———, uncontrolled field; · · ·, three secondary sources located at (−1.4, −0.9, −0.4), (0.15, 0.15, 0.15) and (−0.8, −0.7, −0.35); – · –, two secondary sources located at (−1.4, −0.9, −0.4) and (0.15, 0.15, 0.15); - - -, one secondary source located at (−1.4, −0.9, −0.4).

Figure 8 shows the effect of boundary conditions on noise control. Suppose that there is one primary source and one secondary source in the enclosure. J is chosen as the cost function. Three sensors are used in this case. Two types of impedance z_n ($10^5/k + 10i$ and $10/k + 10i$), are chosen in this case to represent different levels of wall absorptivity. For the case of $z_n = 10^5/k + 10i$, the maximum reduction is 37.49 dB ($k = 2.1$) and the average reduction for the range of wave number $k = 0.5$–4 is 6.74 dB/Hz, while for the case of $z_n = 10/k + 10i$, the maximum reduction is 13.64 dB ($k = 2.3$) and the average reduction for the range of wave number $k = 0.5$–4 is 4.81 dB/Hz. Larger acoustic resistance amounts to smaller absorptivity at the boundary, provided the acoustic reactance is maintained constant. Since a rigid boundary usually results in higher pressure resonant peaks, there is apparently more room to attenuate the noise field.

Vehicle cabin

A vehicle cabin is selected as a more realistic case to verify the optimal active and passive noise control techniques. BEM is particularly suited for

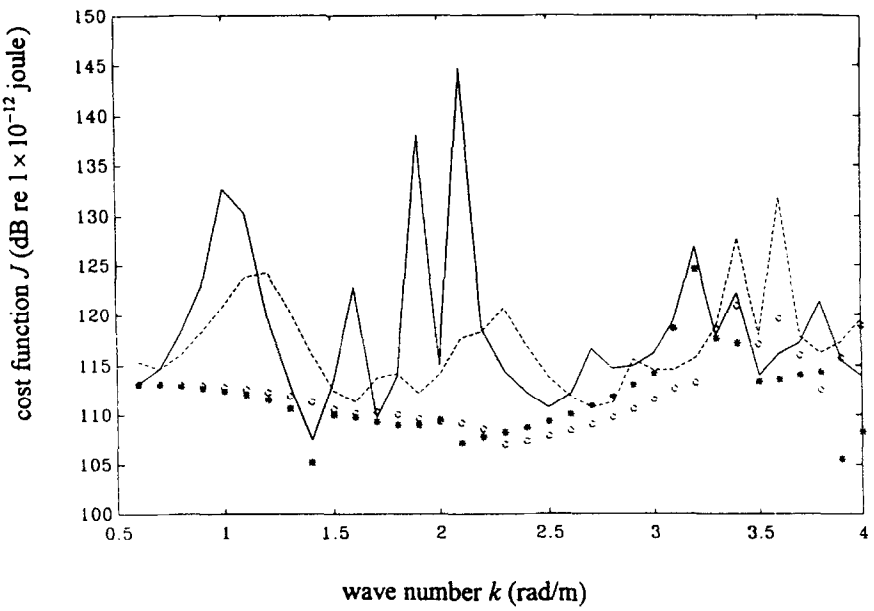

Fig. 8. The effect of boundary conditions of the rectangular enclosure. The primary source of unity amplitude is located at (1.0, 0.2, 0.2). The secondary source is located at (−1.4, −0.9, −0.4). Three sensors are located at (1.4, 0.95, 0.45), (1.0, 0.4, 0.2) and (0.2, 0.1, 0.1). ———, uncontrolled field with boundary impedance $z_n = 10^5/k + 10^5 i$; ∗, controlled field with boundary impedance $z_n = 10^5/k + 10^5 i$; - - -, uncontrolled field with boundary impedance $z_n = 10^5/k + 10^5 i$; ○, controlled field with boundary impedance $z_n, = 10^5/k + 10^5 i$.

modeling the acoustic field, since no analytical solution is available for this irregularly shaped enclosure. Since the geometry of the cabin is more complex than the forgoing rectangular enclosure, more elements are required to construct BEM mesh (90 elements with 272 nodes), as shown in Fig. 9. In the simulation, the impedance of the original boundary without any treatment is assumed to be $10^5/k + 10^5 i$. The primary source of unity amplitude is located at (1.25, 1.14, 0.34). Because the space is limited and no information can be added besides that addressed in the case of the rectangular enclosure, only the representative results are given here.

In the ANC case, it is desired to attenuate the noise field in the cabin by means of two secondary sources and three sensors, as shown in Fig. 10. J is chosen as the cost function. To save CPU time, only direct matrix inversion is used to determine the optimal amplitudes of the secondary sources. Fig. 11 shows the ANC results plotted against wave numbers. As in the case of the rectangular enclosure, significant noise reductions are found near the resonant frequencies.

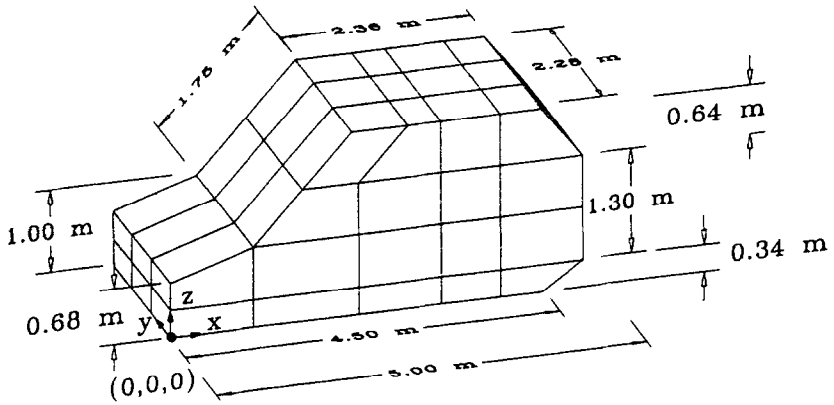

Fig. 9. Dimensions and BEM mesh of the vehicle cabin.

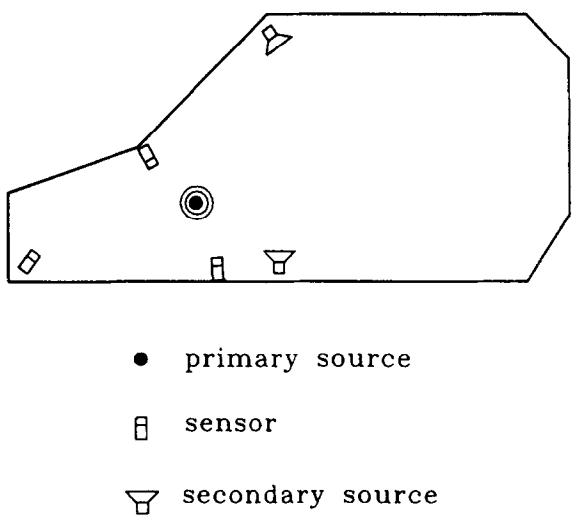

Fig. 10. The positions of the primary source, secondary sources and sensors in the vehicle cabin. The primary source is located at (1.25, 1.14, 0.34). Three sensors are located at (0.15, 0.2, 0.2), (1.25. 0.2, 0.2) and (0.95, 0.2, 0.8). The secondary sources are located at (2.7, 1.10, 0.15) and (2.1, 1.10, 2.28).

CONCLUSION

Boundary-element-method-based optimization techniques have been developed in this study to investigate noise control problems. The methods prove to be effective in solving the optimization problems for active noise control of harmonic sound fields in three-dimensional enclosures.

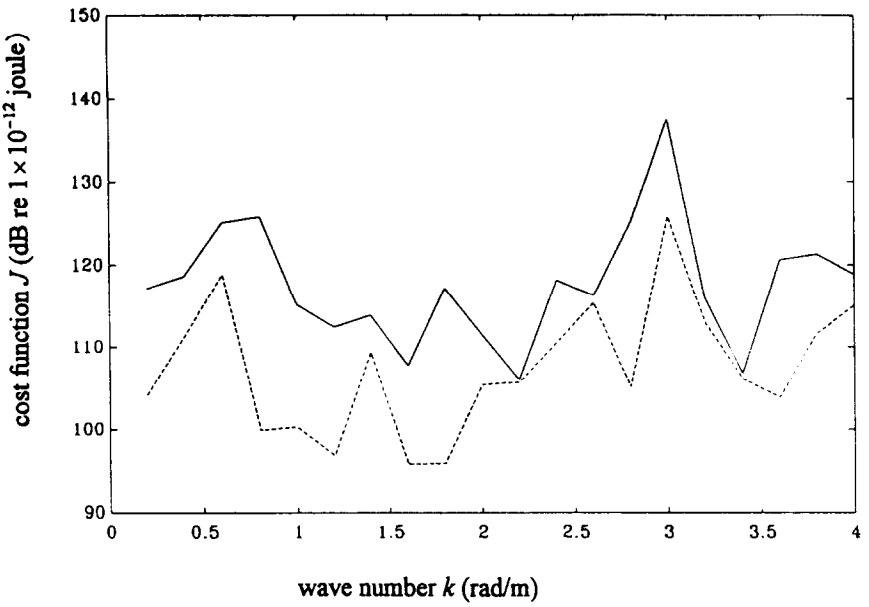

Fig. 11. Noise reduction in the vehicle cabin for different wave numbers by ANC. The boundary impedance z_n is $10^5/k + 10^5 i$. The primary source of unity amplitude is located at (1.25, 1.14, 0.34). Three sensors are located at (0.15. 0.2, 0.2), (1.25, 0.2, 0.2) and (0.95, 0.2, 0.8). The secondary sources are located at (2.7, 1.10, 0.15) and (2.1, 1.10, 2.28). ———, the uncontrolled field; - - -, the controlled field.

Under the constraints that the positions of sources should be confined within the enclosure and the amplitudes of secondary sources should not exceed a certain limit, the CSD method provides optimal positions and amplitudes of secondary sources that minimize the total time-averaged acoustic potential energy. If no constraint on the distance between the primary source and the secondary source is imposed, the resulting two sources will become a dipole that has poor radiation efficiency at low frequencies.

The result of simulation also indicates that the sensors should be located in the pressure anti-nodes for good observability. Significant noise reductions can usually be obtained near resonant frequencies. The mean-square pressures obtained by a discrete number of sensors serve as a useful cost function of local quiet zones. The secondary sources should be located near the pressure anti-nodes to have good controllability on the noise field in the enclosure. In general, the more the secondary sources, the better is the controllability. The techniques are also tested on a vehicle cabin of complex geometry. Satisfactory results have been obtained for the optimization problem. The conclusions drawn from the rectangular enclosure remain applicable here.

ACKNOWLEDGEMENTS

The work was supported by the National Science Council in Taiwan, under the project number NSC-81-0401-E009-571.

REFERENCES

1. Nelson, P. A. & Elliott, S. J., *Active Control of Sound.* Academic Press, New York, 1992.
2. Nelson, P. A. & Elliott, S. J., The minimum power output of a pair of free field monopole sources. *J. Sound Vib.*, **105** (1986) 173–8.
3. Tohyama, M. & Suzuki, A., Active power minimization of a sound source in a closed space. *J. Sound Vib.*, **119** (1987) 562–4.
4. Nelson, P. A., Curtis, A. R. D., Elliott, S. J. & Bullmore, A. J., The minimum power output of free field point sources and the active control of sound. *J. Sound Vib.*, **116** (1987) 415–26.
5. Nelson, P. A., Curtis, A. R. D., Elliott, S. J. & Bullmore, A. J., The active minimization of harmonic enclosed sound fields, Part I. *J. Sound Vib.*, **117** (1987) 1–13.
6. Elliott, S. J., Joseph, P., Nelson, P. A. & Johnson, M. E., Power output minimization and power absorption in the active control of sound. *J. Acoust. Soc. Am.*, **90** (1991) 2501–12.
7. Cunefare, K. A. & Koopmann, G. H., Global optimum active noise control: surface and far-field effects. *J. Acoust. Soc. Am.*, **90** (1991) 365–73.
8. Molo, G. & Bernhard, R. J., Generalized method of predicting optimal performance of active noise controllers. *AIAA J.*, **27** (1989) 1473–8.
9. Molo, G. & Bernhard, R. J., Numerical evaluation of the performance of active noise control systems. *ASME J. Vibr. Acoust.*, **112** (1990) 230–6.
10. Pierce, A. D., *Acoustics.* McGraw-Hill, New York, 1981.
11. Banerjee, P. K. & Butterfield, R., *Boundary Element Methods in Engineering Science.* McGraw-Hill, New York, 1981.
12. Luenberger, D. G., *Linear and Nonlinear Programming.* Addison Wesley, Reading, MA, 1984.
13. Arora, J. S., *Introduction to Optimum Design.* McGraw-Hill, New York, 1989.